http://www.trakya.edu.tr/Enstituler/FenBilimleri/fenbilder/index.php
Trakya Univ J Sci, 6(1): 1-11, 2005
ISSN 1302 647X
DIC: 127JMGB610406040704

Research Article/Araştırma Makalesi

MACHINING OF HYPOCYCLOIDAL SURFACES BY ADDING ROTATIONS AROUND PARALLEL AXES, PART I: KINEMATICS OF THE METHOD AND RATIONAL FIELD OF APPLICATION

Jordan MAXIMOV, Hristo HRISTOV
Faculty of Mechanical Engineering, Technical University of Gabrovo, 5300 Gabrovo, Bulgaria, Tel: 35966 801222, e-mail: maximov@tugab.bg

Received : 28.01.2004
Accepted : 06.07.2004

Abstract: This article presents a method of machining hypocycloidal internal and external polyhedral surfaces by adding rotations around parallel axes. This method can be employed on lathes, drilling and milling machines and machining centers, which significantly broadens their manufacturing capabilities. The kinematics of the method has been defined from the point of view of the design engineer of tools with a view to developing a generalized model of the cutting angles during the machining of hypocycloidal surfaces by adding rotations around parallel axes. The rational field of application of this method has been determined.

Key words: Cutting; cutting tools; hypocycloidal surfaces; machining methods; polygon shaft joints; tool angles.

Paralel eksenlere dönme ekleyerek hypocycloid yüzeylerin talaşlı işlenmesi: Bölüm 1: takım gövdesinin geometrisi

Özet: Bu makalede paralel eksenlere dönme ilave ederek hypocycloid iç ve polihedral dış yüzeylerin talaşlı işlenmesinde kullanılan takım geometrisi sunuldu. Paralel eksenlere dönme ilave edilerek hypocycloid yüzeylerin talaşlı işlenmesinde temel kesme açıları matematiksel olarak modellendi. Elde edilen model kesici takımın kullanılabilir dizaynına müsade ederken, bahsedilen yöntemin mekanik diyağramlar arsındada kalmasını sağlar.

Anahtar kelimeler: Kesme, Kesme takımları, Hypocycloid yüzeyler, talaşlı işleme yöntemleri, poligon şaft bağlantıları, kesme açıları

Introduction

Forming by cutting of cross-profile surfaces can be implemented mostly by two methods:

- Three-dimensional copying method;
- Generating method.

The implementation of the first method requires a special cutting machine, for example a broaching machine. In this aspect, the implementation of the second method allows a bigger freedom of choice of machine tools, including conventional machines.

In the general case, the formation tool motion related to the fixed workpiece of the second method is a superposition of complicated rotation and translation along the axis of the hole being formed. The rotation is around an instantaneous axis of rotation (IAR). The trajectories of the IAR in a coordinate system fixed to a workpiece is an axoid. When this axoid is a upright round cone or a upright round cylinder the case implementation is the simplest. In this case the complicated rotation is round coplanar axes, concurrent or parallel, respectively. The adding rotations around intersecting axes is a basis of the mechanics of the method of cold hole expansion, called spherical mandrelling (Maximov, 2002a; Maximov, 2002c; Maximov and Anchev, 2003a; Maximov and Kalchev, 2003b; Maximov, 2003c; Maximov, 2004) and of the method of forming of cross-profile holes by simultaneous cutting and surface plastic deformation, called spherical broaching and mandrelling (Maximov, 1990; Maximov, 2002b).

Particular cases of forming square holes in fixed workpieces on machine tools with rotating primary motion, for which the tool and hole axes are parallel, are known. The holes are previously drilled cylindrically. The tool (Gardner, 1969) has an oval trihedral shape and carries out both rotating and feeding axial motion but its axis of rotation does not coincide with the symmetry axis of the square hole, and it circumscribes a cylindrical surface. This complicated motion is obtained by fixing the tool in a special floating chuck which is directed by a jig bush during rotation.

The shortcomings of this method are: its low efficiency, because of the magnitude constraints to the machine spindle angular velocity; impact load on the cutting edges of the tool; noisy performance; special floating chuck should be used.

Particular cases of forming external and internal cross-profile surfaces are known when the tool (lathe tool) is fixed to a satellite wheel, rotating around parallel axes in a planetary gear mechanism with spur gears (Borenshteyn, 1978; Radev and Kolev, 1982). These particular applications do not offer the opportunity of using a multi-point tool with a view of enhancing productivity and improving the dynamics of the technological system.

In the indicated cases the primary tool motion with respect to the fixed workpiece is a sum of rotations around parallel axes, but these cases are not subordinated and theoretically well-grounded in the general method. The primary tool motion is planar: rolling of a mobile centroid (a circumference) along a stationary centroid (also a circumference). Therefore the trajectories of points of the tool cutting edges are a kind of cycloids and hence a priori the obtained holes have cycloidal profiles.

On the basis of the formulated and proved theorem (Maximov, 2003c) specifying a necessary and sufficient condition of forming a hypocycloidal n-gon when rotating the linear (n-1)-gon around two parallel axes a method of manufacturing of hypocycloidal internal and external polyhedral surfaces in stationary as well as in rotating workpieces has been synthesized by adding up rotations around parallel axes. This method can be employed on lathes, drilling and milling machines and machining centers, which significantly broadens their manufacturing capabilities.

The vertices of the cutting edges in the primary motion of the tool describe a hypocycloide in the workpiece coordinate system. The velocities of these points are periodic vector functions changing both in size and in direction. Therefore the cutting angles in the primary motion will be scalar functions of the time. The presence of these functions is a necessary condition for determination of the tool geometry.

The objective of the first part of this study is to define the kinematics of the method from the point of view of the design engineer of tools with a view to developing a generalized model of the cutting angles during the machining of hypocycloidal surfaces by adding rotations around parallel axes and to determine the rational field of application of this method.

The following basic tasks have been solved as a result of the whole investigation:

- The kinematics of the method has been defined from the point of view of the design engineer of tools;
- The rational field of application of the method has been determined;
- Generalized model of the cutting angles during the machining of hypocycloidal surfaces by adding rotations around parallel axes has been developed.

Nature of the method of machining hypocycloidal surfaces by adding rotations around parallel axes

Figure 1 shows the kinematics of the proposal method. The essence of the method is that the tool 3 besides axial displacement at velocity $\vec{f}$ performs rotation around its own axis at angular velocity $\vec{\omega}_r$ and at the same time rotates around the axis of symmetry of the n - hedron (inner 2 or outer 1) being machined, at angular velocity $\vec{\omega}_e$ with respect to the static workpiece. The angular velocities have opposite directions and $|\omega_r| > |\omega_e|$ and the absolute angular velocity is the vector sum $\vec{\omega}_a = \vec{\omega}_e + \vec{\omega}_r$. The ratio of the magnitudes of the angular velocities is:

$$\frac{\omega_e}{\omega_r} = -\frac{n-1}{n} \qquad (1)$$

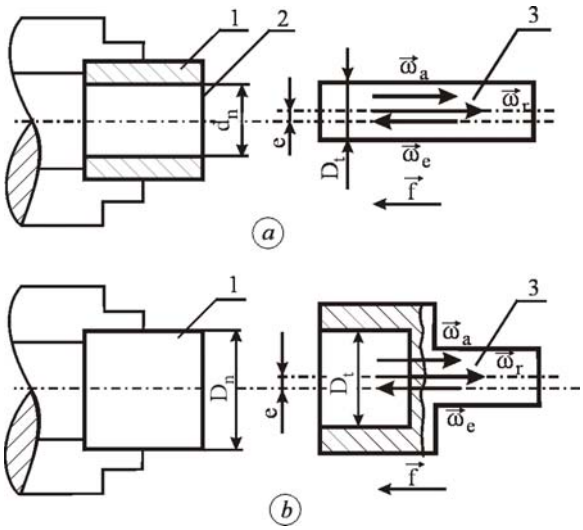

Figure 1. Kinematic diagram of the proposal method: a. machining of inner hypocycloidal surfaces; b. machining of outer hypocycloidal surfaces

The distance between the axes of the tool and the hypocycloidal n - hedron being machined is:

$$0 < e < e_{lim} \tag{2}$$

where e_{lim} is the magnitude of excentricity for which the curvature at the corners of the hypocycloidal n-hedron is infinitely large.

The number of cutting edges of the tool is $(n-1)$. The diameter D_t of the circumference circumscribed around them is:

$$D_t = D_n - 2e \tag{3}$$

If the tool-workpiece system is given angular velocity $-\vec{\omega}_e$, the method can be adapted on lathes where the workpiece and the tool carry out simple rotations around their own axes. The workpiece rotates at angular velocity $\vec{\omega}_1 = -\vec{\omega}_e$, and the tool – at angular velocity $\vec{\omega}_r$. Both angular velocities are unidirectional and $\frac{\omega_1}{\omega_r} = \frac{n-1}{n}$. At the same time the tool carries out a rectilinear translation along its axis.

Using one and the same device, at identical cutting conditions, outer and inner hypocycloidal polyhedrons of identical geometric parameters can be machined. This makes the method especially suitable for machining hypocycloidal joints.

Kinematics of the method

The primary motion of cutting performed by the tool with respect to the fixed workpiece is planar – a sum of rotations around parallel axes. For a rational choice of the geometric parameters of the tool cutting wedges, it is necessary to know the law of motion of a point from the circumference passing through the vertices of the cutting edges. In this paper this circumference is referred to as mobile and the circumference circumscribed around the hypocycloidal profile is referred to as stationary.

Trajectories of the vertices of the cutting edges

Figure 2 shows a scheme for determination of the trajectories of the vertices of the cutting edges. When the tool axis rotates around the axis of the polyhedron being machined at 2π radians $(\varphi_e = 2\pi)$, the absolute an-

gle of the tool rotation is $\varphi_a = \frac{2\pi}{n-1}$. Each cutting edge forms more than one side of the polyhedron in cross section. Its profile is composed of the trajectories of vertices M_i of $(n-1)$- gon, coinciding with the vertices of the cutting edges of the tool when it rotates at angle $\varphi_a = \frac{2\pi}{n-1}$. Coordinate system $x_1 y_1$ is fixed to the tool.

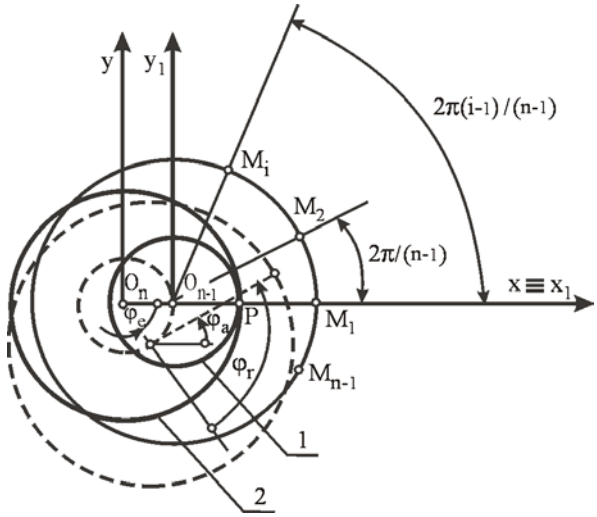

Figure 2. A diagram for determination of the trajectories of the points M_i

The equations of motion of points M_i and their trajectories in parametric form in the stationary coordinate system xy are obtained from the transformation:

$$[x \;\; y]^T = [T][e \;\; x_1 \;\; y_1]^T \tag{4}$$

where:

$$[T] = \begin{bmatrix} \cos\varphi_e & \cos\frac{\varphi_e}{n-1} & -\sin\frac{\varphi_e}{n-1} \\ -\sin\varphi_e & \sin\frac{\varphi_e}{n-1} & \cos\frac{\varphi_e}{n-1} \end{bmatrix} \tag{5}$$

is a transforming matrix,

$$[e \;\; x_1 \;\; y_1]^T = \begin{bmatrix} e & \frac{D_t}{2}\cos\alpha_i & \frac{D_t}{2}\sin\alpha_i \end{bmatrix}^T \tag{6}$$

is an enlarged vector of point M_i coordinates in $x_1 y_1$,

$$\alpha_i = \frac{2\pi}{n-1}(i-1)$$
$$\varphi_e = \omega_e t \in [0, 2\pi]\,; \; i \in [1, (n-1)]\,. \tag{7}$$

From (4)-(6) for the trajectories of points M_i in parametric form in xy is obtained:

$$x = e\cos\varphi_e + \frac{D_t}{2}\cos\alpha_i \cos\frac{\varphi_e}{n-1} - \frac{D_t}{2}\sin\alpha_i \sin\frac{\varphi_e}{n-1}$$
$$y = -e\sin\varphi_e + \frac{D_t}{2}\cos\alpha_i \sin\frac{\varphi_e}{n-1} + \frac{D_t}{2}\sin\alpha_i \cos\frac{\varphi_e}{n-1} \quad (8)$$

The curve (8) has been obtained as a result of rolling the circumference of the mobile centroid 1 along the circumference of the stationary centroid 2 having equations, respectively:

$$x^2 + y^2 = (e\,n)^2 \quad (9)$$

$$x_1^2 + y_1^2 = (n-1)^2 e^2 \quad (10)$$

Therefore points M_i circumscribe $(n\text{-}1)$ number of parts of the elongated hypocycloid which is a theoretical profile of the hypocycloidal n-hedron being obtained. Hypocycloidal n-hedrons can also be machined by a single-point tool. In this case, however, the profile will be formed when rotating tool axis around the polyhedron axis, not at 2π, but at $2\pi(n\text{-}1)$ radians, respectively the productivity will be $(n\text{-}1)$ times lower.

Curvature of the hypocycloidal profile

To determine the function of the curvature of the faces of the hypocycloidal polyhedron, the trajectory of point M1 from Fig. 2 has been studied with equations:

$$x = e\cos\omega_e t + \frac{D_t}{2}\cos\frac{\omega_e t}{n-1}$$
$$y = -e.\sin\omega_e t + \frac{D_t}{2}\sin\frac{\omega_e t}{n-1} \quad (11)$$

where $\omega_e t = \varphi_e$.

The upper curve is an elongated hypocycloid. Its curvature χ is a relationship of the normal acceleration of point M1 and its velocity squared:

$$\chi = \frac{|\ddot{y}\,\dot{x} - \ddot{x}\,\dot{y}|}{\left(\dot{x}^2 + \dot{y}^2\right)^{\frac{3}{2}}} \quad (12)$$

From (12) and (11) for $\chi(\varphi_e)$ is obtained:

$$\chi(\varphi_e) = \frac{\left|\frac{D_t^2}{4(n-1)^3} - e^2 + \frac{eD_t(n-2)}{2(n-1)^2}\cos\frac{n\varphi_e}{n-1}\right|}{\left(e^2 + \frac{D_t^2}{4(n-1)^2} - \frac{eD_t}{n-1}\cos\frac{n\varphi_e}{n-1}\right)^{\frac{3}{2}}} \quad (13)$$

where $\varphi_e \in \langle 0,\ 2\pi \rangle$.

The curvature is the largest at the corners of the hypocycloidal n-hedron. The limit value e_{lim} of the excentricity e is obtained after putting $\varphi_e = 0$ and the denominator of (13) to zero:

$$e_{lim} = \frac{D_t}{2(n-1)} = \frac{D_n}{2n} \quad (14)$$

When $e > e_{lim}$ the curve (11) obtains double points.

The value of e, for which the curvature in the middle of the side of the hypocycloidal n-gon is zero, is:

$$e = e_0 = \frac{D_t}{2(n-1)^2} = \frac{D_n}{2\left[1+(n-1)^2\right]} \tag{15}$$

When $e \in (0, e_0)$ the hypocycloidal profile is convex and when $e \in \langle e_0, e_{lim}) $ two points of each side exist in which the curvature changes its sign.

It is substituted:

$$e = kD_n \tag{16}$$

From (14)-(16) it follows:

- When $0 < k < k_0 = \frac{1}{2\left[1+(n-1)^2\right]}$ the hypocycloidal profile is convex (Fig. 3);
- When $k = k_0$ the curvature in the middle of the side of the hypocycloidal n-gon is zero;
- When $k_0 < k < k_{lim} = \frac{1}{2n}$ two points of each side exist in which the curvature changes its sign.;
- When $k = k_{lim}$ the curvature at the corners obtains an infinitely large value;
- When $k > k_{lim}$ the contour of the profile obtains double points.

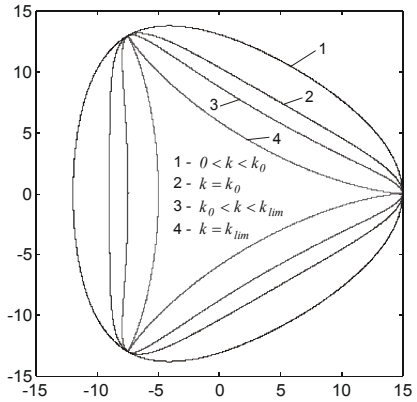

Figure 3. Dependence of hypocycloidal profile on k

Cutting speed in the primary motion

From (11) and (16) for the speed projection on the fixed axes is obtained:

$$v_x = \dot{x} = -D_n\,\omega_e\left[k\sin\omega_e t + \frac{1-2k}{2(n-1)}\,\sin\frac{\omega_e t}{n-1}\right]$$

$$v_y = \dot{y} = D_n\,\omega_e\left[-k\cos\omega_e t + \frac{1-2k}{2(n-1)}\,\cos\frac{\omega_e t}{n-1}\right] \tag{17}$$

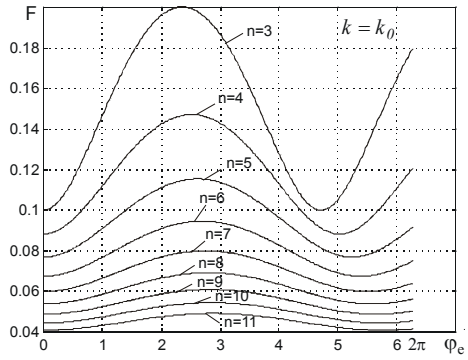

Figure 4. Dependence of the F-function on φ_e

The cutting speed in the primary motion is a vector function of the rotating angle φ_e of the tool axis around the hole axis. Its magnitude (in m/min) is:

$$v = 2\pi\, n_e D_n F(\varphi_e) \tag{18}$$

where

$$F(\varphi_e) = \sqrt{\left[k\sin\varphi_e + \frac{1-2k}{2(n-1)}\,\sin\frac{\varphi_e}{n-1}\right]^2 + \left[-k\cos\varphi_e + \frac{1-2k}{2(n-1)}\,\cos\frac{\varphi_e}{n-1}\right]^2} \tag{19}$$

and n_e in tr/min is the rotation frequency of the tool axis around the hole axis , and D_n is in m. The function $F(\varphi_e)$ is graphically illustrated in Fig. 4.

The variable angle $\theta = \theta(\varphi_e)$ is between the speed vector $\vec{v}$ and the tangent at the same point to the mobile circumference (Fig. 5). The change in the static cutting angles in the principal motion is due to the function $\theta = \theta(\varphi_e)$ and therefore the knowledge of this function is of the utmost importance for defining the geometry of the tool cutting wedges. From Fig. 5 it follows for $\theta = \theta(\varphi_e)$:

$$\theta = \frac{\pi}{2} - \varphi_a - \psi \tag{20}$$

where

$$\varphi_a = \frac{\varphi_e}{n-1}\;; \qquad \psi = \operatorname{arctg}\frac{\dot{y}}{|\dot{x}|} \tag{21}$$

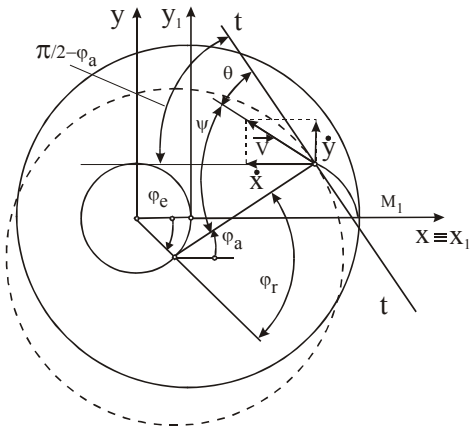

Figure 5. A diagram for determination of the trajectories of the kinematic angle θ

From (21), (17) and (20):

$$\theta = \frac{\pi}{2} - \frac{\varphi_e}{n-1} - \operatorname{arctg} \frac{-k\cos\varphi_e + \frac{1-2k}{2(n-1)}\cos\frac{\varphi_e}{n-1}}{k\sin\varphi_e + \frac{1-2k}{2(n-1)}\sin\frac{\varphi_e}{n-1}} \tag{22}$$

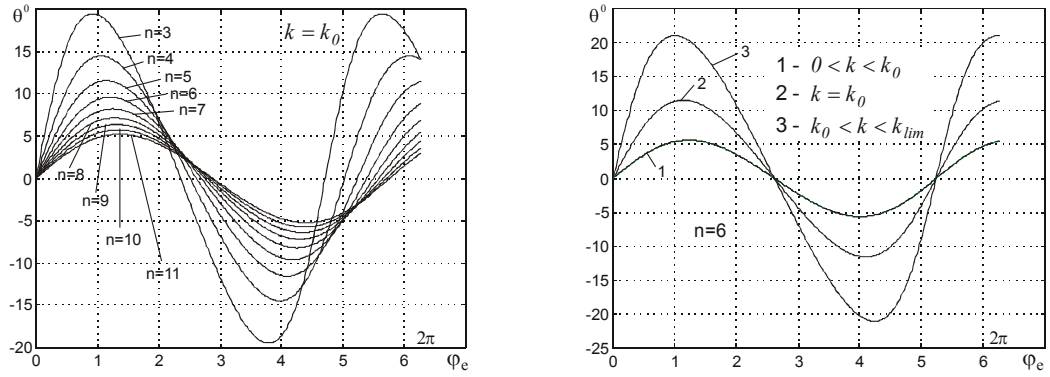

Figure 6. Dependence of θ on φ_e

Fig. 6 shows graphically the function $\theta = \theta(\varphi_e)$. It does not depend on the absolute value of the geometric parameters e and D_n, and only on their relation and on the number of faces n.

Rational field of application of the method

The field of the method application is restricted by the maximum value $\theta_{max} = \theta^*$ of the kinematic angle θ (relationship (22)). The parameters on which θ^* depends are k and n. Although there is a correlation between them which defines characteristic shapes of the hypocycloidal profile, they could be assumed to be independent parameters of the function $\theta^* = \theta^*(k, n)$. The latter is obtained from (22). To this end, its argument

$\varphi_e = \varphi^*(k,n)$, which maximizes (22) is approximated numerically in a suitable manner, as a function of k and n. The investigation of (22) shows that n has a stronger impact on $\varphi_e = \varphi^*(k,n)$ compared to k, and therefore:

$$\varphi^* = -0.007n^2 + 0.157n + 0.492 \tag{23}$$

From (22) and (23):

$$\theta^*(k,n) = \frac{\pi}{2} - \frac{\varphi^*}{n-1} - \operatorname{arctg}\frac{-k\cos\varphi^* + \frac{1-2k}{2(n-1)}\cos\frac{\varphi^*}{n-1}}{k\sin\varphi^* + \frac{1-2k}{2(n-1)}\sin\frac{\varphi^*}{n-1}} \tag{24}$$

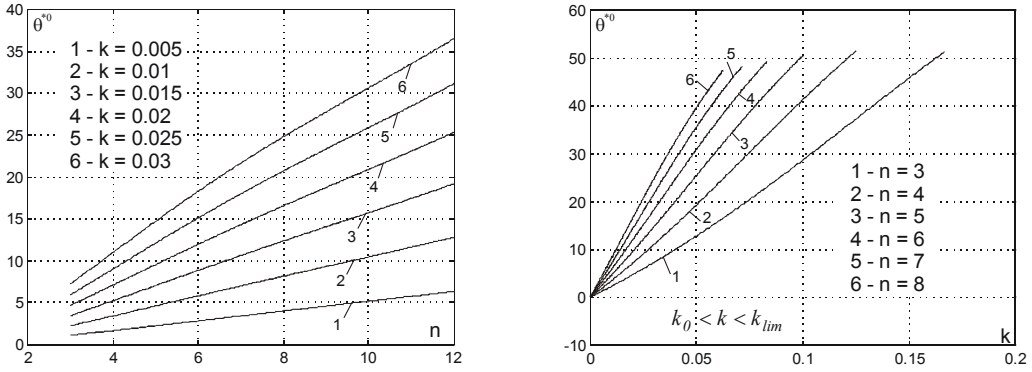

Figure 7. Dependence of θ^* on n and k

Figure 7 shows the impact of k and n (considered as independent parameters) on θ^* and each combination of k and n defines a concrete hypocycloidal profile. However, when θ^* is to be juxtaposed for hypocycloidal profiles with equal convexity (e. g. k=k0), differing only in the number of sides n, then the correlation between k and n has to be taken into account (Fig. 8). It is seen from that in this case when the number n of sides increases, θ^* decreases exponentially.

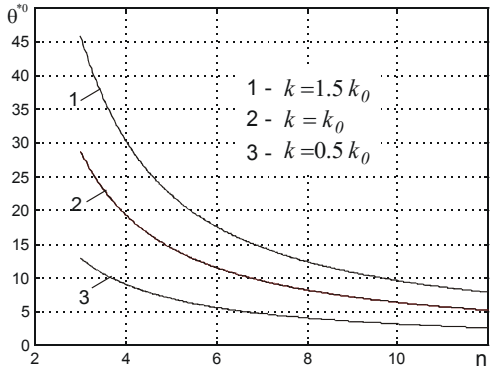

Figure 8. Dependence of θ^* on n with a correlation between k and n

The increase in θ^* deteriorates the cutting process: the change in the cutting angles in the principal motion of the tool increases as well as the cutting speed irregularity. Therefore, a trade-off optimum region should be

found in plane k n, which should define the set of combinations between k and n, for which θ^* does not exceed a preset value.

The governing parameters vector is :

$$\{X\} = [k \;\; n]^T \tag{25}$$

The parametric constrains are:

$$3 \le n \le n_{max} \tag{26}$$

The functional constraints are determined by characteristic values of k, respectively k_0 and k_{lim} :

$$0 < k < \frac{1}{2\left[1 + (n-1)^2\right]} \tag{27}$$

for hypocycloidal surfaces of convex profile;

$$\frac{1}{2\left[1 + (n-1)^2\right]} \le k \le \frac{1}{2n} \tag{28}$$

for hypocycloidal surfaces of concave profile.

The geometric loci of points $\theta_i^*(k_i,\ n_i)$, where the function $\theta^* = \theta^*(k, n)$ assumes constant values are called level lines. They are obtained from (24) after putting $\theta^* = const$ and solving with respect to k:

$$k(n) = \frac{0.5}{1 + F(n)} \tag{29}$$

where:

$$F(n) = \frac{F_1(n) + F_2(n)}{F_3(n) - F_4(n)}\ ;\quad F_1(n) = (n-1)\sin\varphi^*\ ;\quad F_2(n) = (n-1)\ \cos\varphi^*\ \mathrm{tg}\left(\frac{\varphi^*}{n-1} + \theta^*\right)$$

$$F_3(n) = \cos\frac{\varphi^*}{n-1}\ \ \mathrm{tg}\left(\frac{\varphi^*}{n-1} + \theta^*\right);\quad F_4(n) = \sin\frac{\varphi^*}{n-1}$$

and φ^* is found from (23).

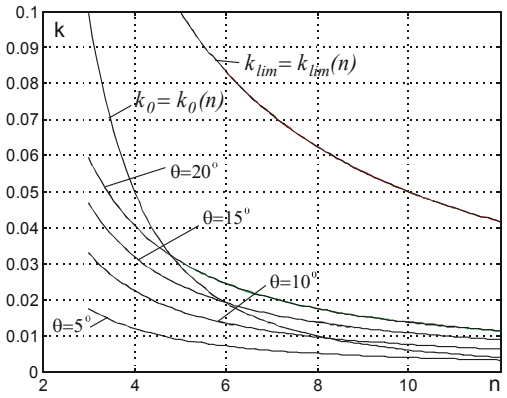

Figure 9. Rational field of application of the method for various level lines θ^*

In Fig 9 in plane kn trade-off optimum regions are shown for various level lines θ_i^* for $n_{max} = 12$, from which rational combinations of k and n can be found depending on the preset value of θ^*. For instance, for $\theta^* \le 5^0$ in the interval $3 \le n \le 12$ only hypocycloidal surfaces with convex profiles can be machined, whereas when $\theta^* = 10^0$ only for $n \ge 9$ hypocycloidal surfaces with concave profile can be machined, etc.

Conclusions

A method of machining hypocycloidal internal and external polyhedral surfaces by adding rotations around parallel axes has been presented. This method can be employed on lathes, drilling and milling machines and machining centers, which significantly broadens their manufacturing capabilities.

The kinematics of the method has been defined and a rational field of application has been determined.

The utilization of the method on lathes is particularly effective. Using one and the same device, at identical cutting conditions, outer and inner hypocycloidal polyhedrons of identical geometric parameters can be machined. This makes the method especially suitable for machining hypocycloidal joints.

Acknowledgements

This work was supported by the Bulgarian Ministry of Education and the Technical University of Gabrovo under Contract No II-2/2003.

References

1 BORENSHTEYN YP. Mechanisms for reproduction of complex profiles. Moscow, Mashinostroenie, 1978.

2 DRUZHINSKIY IA. Working methods of complex surfaces on machine tools. Moscow, Mashinostroenie, 1965.

3 GARDNER M. The Unexpected Hanging and Other Mathematical Diversions. Simon & Schuster, New York, 1969.

4 MAXIMOV JT. Optimization Method for Metal-forming Processes. Energy, 27(7): 675-701, 2002.

5 MAXIMOV JT. Forming of Cross-profile Holes by Adding Rotations round Coplanar Axes. Int J Machine Tools Manufacture 42: 313-320, 2002.

6 MAXIMOV JT. Spherical Mandrelling Method Implementation on Conventional Machine Tools. Int J Machine Tools Manufacture 42: 1315-1325, 2002.

7 MAXIMOV JT, ANCHEV AP. Modelling of residual stress field in spherical mandrelling. Int J Machine Tools Manufacture 43: 1241-1251, 2003.

8 MAXIMOV JT, KALCHEV GM. Modelling of spherical mandrelling manufacturing resistance. Int J Machine Tools Manufacture 44: 95-100, 2003.

9 MAXIMOV JT. Synthesis, mechanics and thermodynamic optimization of metal-working processes when adding rotation around coplanar axes. DrSc Dissertation, Sofia, 2003.

10 MAXIMOV JT. Kinematic and force analysis of the spherical broaching and mandrelling process. PhD Dissertation, Gabrovo, 1990.

11 MAXIMOV JT. Finite element analysis of the spherical mandrelling process of cylindrical holes. Finite Elements in Analysis Des 40: 1217-1232, 2004.

12 RADEV V, KOLEV P. Machining of polyhedral workpieces on lathes by a kinematic method. Machinostroene, 8: 362-366,1982.